

---

---

# Spillover and Partial-Volume Correction for Image-Derived Input Functions for Small-Animal $^{18}\text{F}$ -FDG PET Studies

Yu-Hua Dean Fang<sup>1,2</sup> and Raymond F. Muzic, Jr.<sup>1-3</sup>

<sup>1</sup>Department of Biomedical Engineering, Case Western Reserve University, Cleveland, Ohio; <sup>2</sup>Case Center for Imaging Research, Case Western Reserve University, Cleveland, Ohio; and <sup>3</sup>Department of Radiology, University Hospitals Case Medical Center, Case Western Reserve University, Cleveland, Ohio

We present and validate a method to obtain an input function from dynamic image data and 0 or 1 blood sample for small-animal  $^{18}\text{F}$ -FDG PET studies. The method accounts for spillover and partial-volume effects via a physiologic model to yield a model-corrected input function (MCIF). **Methods:** Image-derived input functions (IDIFs) from heart ventricles and myocardial time-activity curves were obtained from 14 Sprague-Dawley rats and 17 C57BL/6 mice. Each MCIF was expressed as a mathematic equation with 7 parameters, which were estimated simultaneously with the myocardial model parameters by fitting the IDIFs and myocardium curves to a dual-output compartment model. Zero or 1 late blood sample was used in the simultaneous estimation. MCIF was validated by comparison with input measured from blood samples. Validation included computing errors in the areas under the curves (AUCs) and in the  $^{18}\text{F}$ -FDG influx constant  $K_i$  in 3 types of tissue. **Results:** For the rat data, the AUC error was  $5.3\% \pm 19.0\%$  in the 0-sample MCIF and  $-2.3\% \pm 14.8\%$  in the 1-sample MCIF. When the MCIF was used to calculate the  $K_i$  of the myocardium, brain, and muscle, the overall errors were  $-6.3\% \pm 27.0\%$  in the 0-sample method (correlation coefficient  $r = 0.967$ ) and  $3.1\% \pm 20.6\%$  in the 1-sample method ( $r = 0.970$ ). The  $t$  test failed to detect a significant difference ( $P > 0.05$ ) in the  $K_i$  estimates from both the 0-sample and the 1-sample MCIF. For the mouse data, AUC errors were  $4.3\% \pm 25.5\%$  in the 0-sample MCIF and  $-1.7\% \pm 20.9\%$  in the 1-sample MCIF.  $K_i$  errors averaged  $-8.0\% \pm 27.6\%$  for the 0-sample method ( $r = 0.955$ ) and  $-2.8\% \pm 22.7\%$  for the 1-sample method ( $r = 0.971$ ). The  $t$  test detected significant differences in the brain and muscle in the  $K_i$  for the 0-sample method but no significant differences with the 1-sample method. In both rat and mouse, 0-sample and 1-sample MCIFs both showed at least a 10-fold reduction in AUC and  $K_i$  errors compared with uncorrected IDIFs. **Conclusion:** MCIF provides a reliable, noninvasive estimate of the input function that can be used to accurately quantify the glucose metabolic rate in small-animal  $^{18}\text{F}$ -FDG PET studies.

**Key Words:** input function; spillover correction; partial-volume effect correction; compartment modeling

**J Nucl Med 2008; 49:606-614**

DOI: 10.2967/jnumed.107.047613

**P**ET with  $^{18}\text{F}$ -FDG is widely used to quantify glucose metabolism. This entails compartment modeling to estimate kinetic rate constants and requires knowledge of the input function, which is the  $^{18}\text{F}$ -FDG plasma time-activity curve (1,2). The gold standard to determine the input function is an invasive blood-sampling procedure to measure the  $^{18}\text{F}$ -FDG activity concentration in the arterial blood. For small-animal  $^{18}\text{F}$ -FDG PET studies, this procedure is challenging because of the small size of blood vessels and the limited blood volume. In addition, blood loss may perturb the physiology and confound the experimental outcome. To avoid these problems, various methods have been proposed to estimate the input function noninvasively. Those methods can be categorized as image-derived input functions (IDIFs), factor analysis (FA) methods, standardized input functions, and simultaneous estimation.

IDIFs are the time-activity curves obtained by drawing regions over the major vascular structures, such as the ventricular cavity, aorta, or large arteries (3). In principle, this method is relatively simple to use. However, in small-animal imaging, hearts and arteries are small compared with the scanner spatial resolution. Consequently, vascular radioactivity is blurred into adjacent tissues and vice versa. Also, cardiac and respiratory motion creates additional cross-contamination between vascular structures and surrounding tissues. As a result, curves obtained from regions drawn over the vascular space will be a mixture of the input function and the surrounding tissue time-activity curves. Some methods have been proposed to correct for the mixing—sometimes called spillover and partial-volume effect—in IDIFs using a few blood samples in clinical studies (4,5). For small-animal PET, Yee et al. applied the IDIF method to  $^{15}\text{O}$ -water studies with correction for partial volume and spillover (6). However,

Received Sep. 27, 2007; revision accepted Dec. 20, 2007.

For correspondence or reprints contact: Raymond F. Muzic, Jr., PhD, Radiology, 11100 Euclid Ave., University Hospitals, Cleveland, OH 44106.

E-mail: raymond.muzic@case.edu

COPYRIGHT © 2008 by the Society of Nuclear Medicine, Inc.

the assumption that the blood tracer concentration achieves equilibrium with that in the tissue makes the method inappropriate for  $^{18}\text{F}$ -FDG. Green et al. presented an IDIF in mice assuming a negligible contribution of the myocardium to the cavity curve (7). In many circumstances, this assumption is not valid.

FA methods have been applied to separate the arterial blood and the myocardial tissue components in the dynamic heart images. The heart image is assumed to be a sum of 3 or more factors—typically myocardium and blood in the left and right ventricles. Principal component analysis is applied to find these components and, therefore, obtain an estimate of the input function. FA has been used to extract the input function for rats and mice using just 1 blood sample (8), showing good correlation between the measured and extracted input functions. FA is described as being robust and requiring few blood samples. However, the ambiguity still exists in this method of whether, especially in mice (8), the factors found include the blood curves without spillover and partial-volume degradation. Moreover, an analysis of the consequence of using FA-derived input functions on the  $^{18}\text{F}$ -FDG influx rate constant has not been reported.

Standardized input function methods assume that input functions across animals and experimental conditions have an identical curve shape that can be used to approximate the individual input function by scaling the standard curve to match the concentration measured in 1 or 2 blood samples (9). In reality, the input function curve shape varies between subjects on the basis of several factors, such as the injection technique and speed, dietary state of the animal, metabolic status, catheterization site, and animal species. Therefore, the standard curve lacks the ability to account for the range of curve shapes present, especially in animals with abnormal metabolism. Moreover, the use of standardized input functions has not been validated for mice.

Simultaneous estimation was originally proposed to estimate the input function for human brain studies (10). It is assumed that the input function can be described by a mathematic function with multiple parameters that can be estimated simultaneously with the fitting of multiple regions of interest (ROIs), typically 3. Few, usually 2, late blood samples are required in the simultaneous estimation process. The main challenge of this method is the large number of parameters (>25) that needs to be estimated, thus making the fitting especially challenging. Moreover, this method has not been validated in small-animal PET studies.

In this article we present and validate a method that overcomes the limitations of the above methods. Our method uses simultaneous estimation to correct the spillover and partial-volume effect for an IDIF. We assume that both the IDIF from the heart ventricles and the time–activity curve of the myocardium are mixtures of the true input function and the myocardium uptake. Using a mathematic equation to express the input function, we can then determine both time–activity curves as outputs of a compartment model simultaneously with the nonvascular tissue parameters. The

estimated input is denoted as a model-corrected input function (MCIF) because it is obtained by correcting the spillover and partial-volume effects from IDIF by compartment modeling. This method is validated by comparing the MCIF estimated with 0 or 1 blood sample with the input functions measured with blood sampling in rats and mice. We also compared our MCIF with the uncorrected IDIF.

## MATERIALS AND METHODS

### Rat Studies

All experiments took place in the Case Center for Imaging Research in Case Western Reserve University and were performed according to a protocol approved by its Institutional Animal Care and Use Committee. Twenty datasets were acquired from 14 female Sprague–Dawley rats ranging from 206 to 253 g. Six of the 14 underwent 2 studies separated by 1 wk. For each scan, the rat was anesthetized with 2%–2.5% isoflurane in oxygen. Each rat was cannulated in the tail artery with microrenathane tubing (0.83-mm outer diameter) and in the tail vein with microrenathane tubing (0.63-mm outer diameter). Each microPET study began with a 10-min transmission scan using a  $^{57}\text{Co}$  source on a microPET R4 scanner (Siemens Medical Solutions USA, Inc.). After that, a 90-min emission scan in 3-dimensional data-acquisition mode commenced with the intravenous bolus injection of approximately 30 MBq  $^{18}\text{F}$ -FDG. Dynamic image sequences were reconstructed with 5-s ( $n = 12$ ), 30-s ( $n = 12$ ), 60-s ( $n = 5$ ), and 300-s ( $n = 17$ ) frames. Fourier rebinning and a 2-dimensional filtered backprojection (FBP) algorithm was used for image reconstruction with  $256 \times 256 \times 63$  pixels per frame. Pixel spacing was  $0.42 \times 0.42 \times 1.25$  mm and the field of view included the brain, heart, and lung. Correction for radioactive decay, attenuation, scatter, and dead time was performed during the sinogram histogramming and reconstruction.

Blood sampling was performed to provide a gold-standard reference. For the first 3 min, a continuous automatic blood-sampling device, a blood-activity monitor (BAM), was used to acquire data with a high sampling rate to capture the initial rapid kinetics (11). During this time, the blood was continuously drawn from the arterial line using a syringe pump at 0.2 mL/min flow rate and counted by the BAM using contiguous 0.1-s intervals. After the first 3 min, continuous sampling was discontinued, and 10 samples were manually taken at 3.5, 4, 4.5, 5, 7, 10, 15, 30, 60, and 90 min. For 12 of the 20 studies, a late venous sample at 92 min was taken to compare the activity concentrations in late arterial and venous blood samples. The manual samples were counted with a well counter (Wallac LKB 1282). The sample net weight was measured to obtain the activity concentration from the counts. Input functions from the BAM and manual samples were linearly interpolated to construct a single input function. Shortly after the end of the study, an extra blood sample was taken for determination of the hematocrit and plasma activity fraction (plasma  $^{18}\text{F}$ -FDG divided by whole-blood  $^{18}\text{F}$ -FDG).

### Mouse Studies

In addition to rat data, our method was tested using mouse data shared on the Internet by the Crump Institute of Molecular Imaging, UCLA (12,13). Seventeen C57BL/6 male mice weighing 22–36 g were anesthetized with 1.5%–2% isoflurane in oxygen. Of these, 9 mice were pretreated with insulin. As insulin does not directly affect the spillover and partial-volume effects, these data were treated as 1 group for evaluation of the input function estimation. Into each

mouse, 9–37 MBq  $^{18}\text{F}$ -FDG were bolus-injected in the tail vein. Input functions were measured using femoral artery blood samples. On average, 15 (range, 5–22) samples were collected from each mouse. Eight mice were scanned with a microPET Focus-220 scanner and 9 were scanned with a microPET P4 scanner (both scanners: Siemens Medical Solutions USA, Inc.) For each PET study, a mouse underwent a CT scan for attenuation correction and then either a 60- or 90-min emission scan. Herein, only the first 60 min of data were used to standardize the data analysis. The image reconstruction method was FBP with  $128 \times 128 \times 95$  pixels. Dynamic framing varies slightly among these studies but typically there were 0.5-s ( $n = 15$ ), 2-s ( $n = 1$ ), 4-s ( $n = 1$ ), 6-s ( $n = 1$ ), 15-s ( $n = 1$ ), 30-s ( $n = 3$ ), 60-s ( $n = 1$ ), 120-s ( $n = 1$ ), 180-s ( $n = 3$ ), and 900-s ( $n = 4$ ) frames.

### $^{18}\text{F}$ -FDG Compartment Model

The well-established compartment model has been used for estimating the rate constants and the glucose metabolic rate ( $I, 2$ ). This model entails 2 tissue compartments:  $^{18}\text{F}$ -FDG and phosphorylated  $^{18}\text{F}$ -FDG ( $^{18}\text{F}$ -FDG-6P) in extravascular tissue, denoted by  $C_e$  and  $C_m$ , respectively. The state equations are:

$$\frac{dC_e}{dt} = k_1 C_p - (k_2 + k_3) C_e + k_4 C_m. \quad \text{Eq. 1}$$

$$\frac{dC_m}{dt} = k_3 C_e - k_4 C_m. \quad \text{Eq. 2}$$

The model output equation is:

$$m_i = \frac{\int_{t_b^i}^{t_e^i} (C_e(t) + C_m(t) + F_v \cdot C_a(t)) dt}{t_e^i - t_b^i}, \quad \text{Eq. 3}$$

where  $m_i$  is the model-predicted activity concentration in the  $i$ th frame with the frame beginning at time  $t_b^i$  and ending at time  $t_e^i$ .  $F_v$  is the fraction of the pixel that is vascular space.  $C_p$  and  $C_a$  are the plasma and whole-blood time-activity curves, respectively.  $C_p$  is calculated from  $C_a$  by:

$$C_p(t) = C_a(t) \cdot F_{pa} / (1 - H), \quad \text{Eq. 4}$$

where  $H$  is the hematocrit and  $F_{pa}$  is the fraction of blood activity attributed to that in the plasma (plasma activity divided by whole-blood activity). Although there have been studies showing that the  $F_{pa}$  varies with time ( $14, 15$ ), accounting for this time variation requires blood sampling. In fact, many studies use whole blood as a surrogate for plasma activity and, therefore, implicitly assume that  $F_{pa}$  is constant. Thus, to simplify the procedure and offer the possibility of avoiding blood sampling, we treat  $F_{pa}$  as a constant (We observed  $F_{pa}$  to be  $0.63 \pm 0.07$  in rats.). The glucose metabolic rate of glucose is defined by:

$$MR_{glu} = Ki \cdot C_{glu} / LC. \quad \text{Eq. 5}$$

$LC$  is the lumped constant between  $^{18}\text{F}$ -FDG and glucose, and  $C_{glu}$  is the glucose concentration in blood. The  $^{18}\text{F}$ -FDG influx constant  $Ki$  equals  $k_1 \cdot k_3 / (k_2 + k_3)$ . Often determination of  $Ki$  alone is a sufficient index of glucose metabolism, and it can be robustly estimated. In contrast, obtaining precise estimates of  $k_1$  to  $k_4$  is less frequently used because of parameter correlation and noise in the time-activity curves. Therefore, our present work focuses on the estimates of  $Ki$  in the parameter estimation results.

### Dual-Output Cardiac $^{18}\text{F}$ -FDG Model

Ideally, when an ROI is drawn within the cavity of the left ventricle, the tissue time-activity curve would equal the whole-blood time-activity curve  $C_a$ . However, due to spillover and partial-volume effects, the model-predicted output of an IDIF is more accurately expressed as a mixture of blood and nonvascular tissue activity:

$$m_{IDIF,i} = \frac{\int_{t_b^i}^{t_e^i} [f_c^m (C_e(t) + C_m(t)) + f_c^c \cdot C_a(t)] dt}{t_e^i - t_b^i}, \quad \text{Eq. 6}$$

where  $f_c^m$  is the mixing coefficient from the myocardium to the ventricular cavity, and  $f_c^c$  is the mixing coefficient of the input function  $C_a$ . Similarly, the model output of the surrounding myocardium  $^{18}\text{F}$ -FDG concentration is:

$$m_{myo,i} = \frac{\int_{t_b^i}^{t_e^i} [f_m^m (C_e(t) + C_m(t)) + f_m^c \cdot C_a(t)] dt}{t_e^i - t_b^i}, \quad \text{Eq. 7}$$

where  $f_m^m$  is the mixing coefficient from the tissue  $^{18}\text{F}$ -FDG uptake, and  $f_m^c$  is the mixing coefficient of the input function  $C_a$  contribution to the myocardium ROI. If there is no spillover and partial-volume effect,  $f_m^m$  and  $f_c^c$  would equal 1, and  $f_c^m$  and  $f_m^c$  would equal 0. In microPET images, those 4 mixing coefficients range between 0 and 1, with  $f_m^m$  and  $f_c^c$  dominant (closer to 1) and greater than  $f_c^m$  and  $f_m^c$ . In this study, it is assumed that a single set of extravascular compartments ( $C_e, C_m$ ) is adequate to predict both the ventricular ( $m_{IDIF}$ ) and the myocardial ( $m_{myo}$ ) activities because activities measured in these areas reflect a mixture of the same underlying myocardial extravascular and intravascular activities.

### Simultaneous Estimation

Typical parameter estimation in compartment modeling assumes that both input and output are known, so that model parameters can be estimated by fitting the model output to the experimental data. Simultaneous estimation assumes, however, that the input is unknown but can be described by a model or an equation. Then, both the parameter sets of the input function and the tracer kinetic model can be estimated simultaneously by fitting model outputs to the experimental data. This entails accounting for the dependence of the model output on the input function parameters. In  $^{18}\text{F}$ -FDG PET studies, the input function  $C_a$  can be approximated by a 7-parameter equation ( $16$ ):

$$C_a(t) = \begin{cases} 0, & \text{if } t < \tau \\ (A_1(t - \tau) - A_2 - A_3)e^{L_1(t - \tau)} + A_2e^{L_2(t - \tau)} + A_3e^{L_3(t - \tau)}, & \text{otherwise} \end{cases} \quad \text{Eq. 8}$$

**TABLE 1**  
Initial Values and Bounds for Parameter Estimation to Obtain the MCIF

| Parameter                            | $k_1$<br>(1/min) | $k_2$<br>(1/min) | $k_3$<br>(1/min) | $k_4$<br>(1/min) | $f_m^m$ | $f_c^c$ | $f_m^c$ | $f_c^m$ | $\tau$<br>(min) | $A_1$<br>(MBq/min/mL) | $A_2$<br>(MBq/mL) | $A_3$<br>(MBq/mL) | $L_1$<br>(1/min) | $L_2$<br>(1/min) | $L_3$<br>(1/min) | $w_1$ | $w_2$ | $w_3$ |
|--------------------------------------|------------------|------------------|------------------|------------------|---------|---------|---------|---------|-----------------|-----------------------|-------------------|-------------------|------------------|------------------|------------------|-------|-------|-------|
| <b>Rat</b>                           |                  |                  |                  |                  |         |         |         |         |                 |                       |                   |                   |                  |                  |                  |       |       |       |
| Initial value                        | 0.5              | 1                | 0.1              | 0.001            | 0.9     | 0.95    | 0.4     | 0.4     | 0               | 18.5                  | 0.185             | 0.185             | -7               | -0.1             | -0.015           | 1     | 1     | 0.1   |
| Upper bound                          | 2                | 2                | 0.5              | 0.01             | 1       | 1       | 0.6     | 0.6     | 0.1             | 111                   | 0.74              | 0.555             | -5               | -0.05            | -0.01            | 3     | 3     | 0.1   |
| Lower bound                          | 0                | 0                | 0                | 0                | 0.7     | 0.7     | 0       | 0       | 0               | 0                     | 0                 | 0                 | -20              | -0.5             | -0.02            | 0     | 0     | 0.05  |
| <b>Mouse pretreated with insulin</b> |                  |                  |                  |                  |         |         |         |         |                 |                       |                   |                   |                  |                  |                  |       |       |       |
| Initial value                        | 0.01             | 0.01             | 0.001            | 0.001            | 0.9     | 0.95    | 0.4     | 0.4     | 0               | 111                   | 0.296             | 0.259             | -27              | -0.55            | -0.04            | 1     | 1     | 0.1   |
| Upper bound                          | 0.5              | 0.5              | 0.25             | 0.001            | 1       | 1       | 0.6     | 0.6     | 0.2             | 185                   | 0.333             | 0.259             | -17              | -0.1             | 0                | 3     | 3     | 0.1   |
| Lower bound                          | 0                | 0                | 0                | 0                | 0.7     | 0.7     | 0       | 0       | 0               | 29.6                  | 0.037             | 0.037             | -38              | -2               | -0.04            | 0     | 0     | 0.05  |
| <b>Mouse untreated</b>               |                  |                  |                  |                  |         |         |         |         |                 |                       |                   |                   |                  |                  |                  |       |       |       |
| Initial value                        | 0.01             | 0.01             | 0.001            | 0.001            | 0.9     | 0.95    | 0.4     | 0.4     | 0               | 111                   | 0.296             | 0.259             | -27              | -0.55            | -0.04            | 1     | 1     | 0.1   |
| Upper bound                          | 0.5              | 0.5              | 0.25             | 0.001            | 1       | 1       | 0.6     | 0.6     | 0.2             | 185                   | 0.333             | 0.259             | -17              | -0.1             | 0                | 3     | 3     | 0.1   |
| Lower bound                          | 0                | 0                | 0                | 0                | 0.7     | 0.7     | 0       | 0       | 0               | 29.6                  | 0.037             | 0.037             | -38              | -2               | -0.04            | 0     | 0     | 0.05  |

With Equation 8 and values for  $\tau$ ,  $A_1 \sim A_3$ , and  $L_1 \sim L_3$ , the input function can be approximated and carried into the model for solving the model output  $m_{IDIF}$  in Equation 6 with a given set of  $k_1 \sim k_4$ ,  $f_c^c$ , and  $f_m^m$ . Model output  $m_{myo}$  can be solved in the same way. Model outputs  $m_{IDIF}$  and  $m_{myo}$  are then fit to the corresponding measurements, the PET measurement of  $^{18}\text{F}$ -FDG concentration in the ventricular cavity  $PET_{IDIF}$  and in the myocardium  $PET_{myo}$ , by minimizing the objective function:

$$O(p) = \sum_{i=1}^n \left[ w_1 (m_{IDIF,i} - PET_{IDIF,i})^2 + w_2 (m_{myo,i} - PET_{myo,i})^2 \right], \quad \text{Eq. 9}$$

where  $p$  is the parameter vector  $[\tau, A_1, A_2, A_3, L_1, L_2, L_3, k_1, k_2, k_3, k_4, f_m^m, f_c^c, f_m^c, f_c^m]$  to be optimized.  $n$  is the total number of frames.  $w_1$  and  $w_2$  are weighting coefficients. If 1 blood sample is available to incorporate into the estimation process, the objective function can be extended to:

$$O(p) = \sum_{i=1}^n \left[ w_1 (m_{IDIF,i} - PET_{IDIF,i})^2 + w_2 (m_{myo,i} - PET_{myo,i})^2 \right] + w_3 (C_a(t_s) - b)^2, \quad \text{Eq. 10}$$

where  $b$  is the blood activity concentration at the sampling time  $t_s$ ,  $w_3$  is the weighting associated with the blood sample. The values of the weights  $w_1 \sim w_3$  are estimated simultaneously with all other parameters using an extended least squares (ELS) method described by Muzic and Christian (17). The initial values and the lower and upper bounds of all parameters are summarized in Table 1. Once the simultaneous estimation is finished, the estimated values for parameters  $\tau$ ,  $A_1 \sim A_3$ , and  $L_1 \sim L_3$  are used in Equation 8 to calculate the MCIF.

### VOI and ROI Specification

Heart and myocardium ventricular volumes of interest (VOIs) were drawn for each animal on short-axis slices. When necessary, image volumes were rotated to obtain the short-axis view. A ventricular VOI consisted of 2-dimensional circular ROIs ( $n = 2-4$ ) that were placed on the adjacent slices at the center of the heart ventricular cavity. Those ROIs were approximately 2.1 mm in

diameter for rats and 1.6 mm for mice. A myocardium VOI was made of several 2-dimensional doughnut-like circular ROIs with hollow centers drawn on adjacent slices. The inner diameters of the myocardial ROIs were 4.2 mm for rats and 2.4 mm for mice. The outer diameters were 9.2 mm for rats and 5.2 mm for mice. Figure 1 shows an ROI on rat images. For validation by comparison of Ki values, brain and skeletal muscle ROIs were drawn for each animal.

### Software and Computation Environments

All numeric analyses were done using MATLAB R2007a (Mathworks). Compartment Model Kinetic Analysis Tool (COMKAT) (18), a kinetic modeling toolbox free for noncommercial use, was used for implementing the compartment models and fitting experimental data. The optimization was performed with COMKAT's fitGen function that uses MATLAB function "fmincon," which is based on an interior-reflective Newton method (17,19).

### Input Function Validation

How well an estimated input function approximated the measured input function was determined by direct and indirect methods. The direct method compared input functions by calculating the difference in areas under curves (AUCs) and the root mean square error (RMSE) of estimated input functions. The indirect comparison examined the impact of an estimated input function on the estimated tissue parameter Ki. Ki values in myocardium, brain, and muscle were calculated using a measured input function ( $Ki_{mea}$ ) and an MCIF ( $Ki_{est}$ ). The error percentage

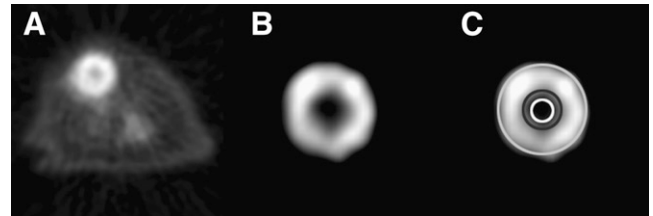


**FIGURE 1.** Illustration of the typical placement of ventricular and myocardium ROIs. (A) The original axial view of rat chest. (B) View of heart after contrast adjustment. (C) The center ROI is the ventricular one. The area between the other 2 ROIs denotes myocardium.

**TABLE 2**  
Direct Comparison of Estimated Input Functions

| Input function      | Species | AUC (MBq·min/mL) | AUC error (%) | RMSE (MBq/mL)   |
|---------------------|---------|------------------|---------------|-----------------|
| Measured            | Rat     | 11.6 ± 3.7       |               |                 |
| IDIF, no correction | Rat     | 25.0 ± 9.4       | 120.7 ± 56.2  | 0.1721 ± 0.0929 |
| MCIF, 0-sample      | Rat     | 11.9 ± 3.8       | 5.3 ± 19.0    | 0.0391 ± 0.0140 |
| MCIF, 1-sample      | Rat     | 11.2 ± 3.7       | -2.3 ± 14.8   | 0.0384 ± 0.0165 |
| Measured            | Mouse   | 4.0 ± 1.4        |               |                 |
| IDIF, no correction | Mouse   | 20.4 ± 11.6      | 412.8 ± 234.8 | 0.2849 ± 0.1805 |
| MCIF, 0-sample      | Mouse   | 4.0 ± 1.7        | 4.3 ± 25.5    | 0.0370 ± 0.0176 |
| MCIF, 1-sample      | Mouse   | 3.9 ± 1.5        | -1.7 ± 21.0   | 0.0345 ± 0.0151 |

AUC error is calculated by  $(AUC_{est} - AUC_{mea})/AUC_{mea} \cdot 100$ . Values are expressed as mean ± SD.

of  $K_i$  was calculated as  $(K_{i_{est}} - K_{i_{mea}})/K_{i_{mea}} \times 100$  for each region and subject. These percent errors were summarized using mean and SD. Also, the correlation coefficients between  $K_{i_{mea}}$  and  $K_{i_{est}}$  were calculated. A  $t$  test with  $\alpha = 0.05$  was used to examine if the  $K_{i_{mea}}$  and  $K_{i_{est}}$  were significantly different in each region.

## RESULTS

Results of the direct comparison between measured input functions, IDIF and MCIF, are summarized in Table 2. As shown in Figure 2, an IDIF without any correction is highly biased because of the spillover. Therefore, the AUC was highly biased and the RMSE was extremely high for the IDIF, as seen in Table 2. For example, the magnitude of AUC errors both in rats and mice exceeded 100%, meaning the AUC was more than double what it should have been. In contrast, under all conditions the MCIF had an AUC error of <6% bias for all conditions—rats and mice, 0 and 1 blood sample. With inclusion of 1 blood sample, this error was about 2%. Thus, compared with the IDIF, the MCIF reduces the AUC error by approximately 20-fold in rats and 100-fold in mice. In terms of RMSE, the MCIF achieved values of about 0.04 MBq/mL, which were much smaller than the 0.17- to 0.28-MBq/mL values obtained with the uncorrected IDIF. To illustrate the input function estimated with 0-sample MCIF compared with the measured input, Figure 3 shows a representative dataset from 1 rat. The input function is accurately estimated for both the early minutes and the whole study, as shown in Figures 3A and 3B, even when the initial guess of the input function parameters is far from the true values. Figure 3C demonstrates that the model output fits the IDIF and myocardium data very well. Figure 4 shows representative fitting results of 1 set of mouse data, indicating the close approximation of the MCIF to the measured input.

As the purpose to estimate the input function is for its use in compartment modeling, evaluating how much error is introduced in the estimates of  $K_i$  is especially important. Table 3 lists the comparison of  $K_i$  values obtained from various input functions. When an IDIF without any correction was used in estimating  $K_i$ , the estimation of  $K_i$  was

highly biased compared with the reference  $K_i$  values obtained using the measured input. This is due to the IDIF itself being highly biased, as shown in the direct comparison described earlier. In contrast, the MCIF greatly reduced the bias in the  $K_i$  estimates. For rats, the overall error percentage of  $K_i$  of all 3 regions averaged  $6.3\% \pm 27.0\%$  for 0-sample MCIF and  $-3.1\% \pm 20.6\%$  for 1-sample MCIF, with correlation coefficients of 0.967 and 0.970, respectively. The  $t$  test failed to detect a significant difference in all 3 types of tissue using either 0-sample or 1-sample MCIF ( $P > 0.05$ ). Comparing the 0-sample and 1-sample MCIF methods, the 1-sample MCIF methods reduced  $K_i$  bias in both the brain and the muscle but slightly increased it in the myocardium. The precision was also greatly improved in the brain and muscle. Correlation coefficients increased in all 3 regions with the 1-sample MCIF. Figure 5 shows a box plot of the  $K_i$  error in 0- and 1-sample MCIF. Including 1 blood sample brought the median value closer to 0 and reduced the interquartile range (IQR). Taken together, these results show that the MCIF performs well in

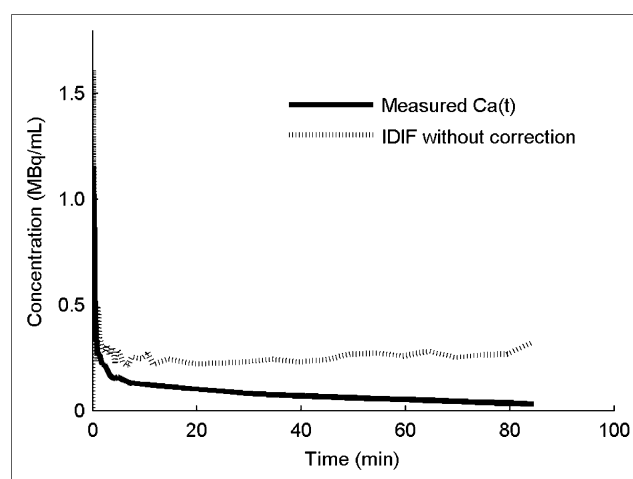


**FIGURE 2.** Comparison between measured input function (solid line) and IDIF (dashed line) in 1 rat shows that the IDIF is higher than the measured input, primarily due to spillover from myocardium  $^{18}\text{F}$ -FDG activity.

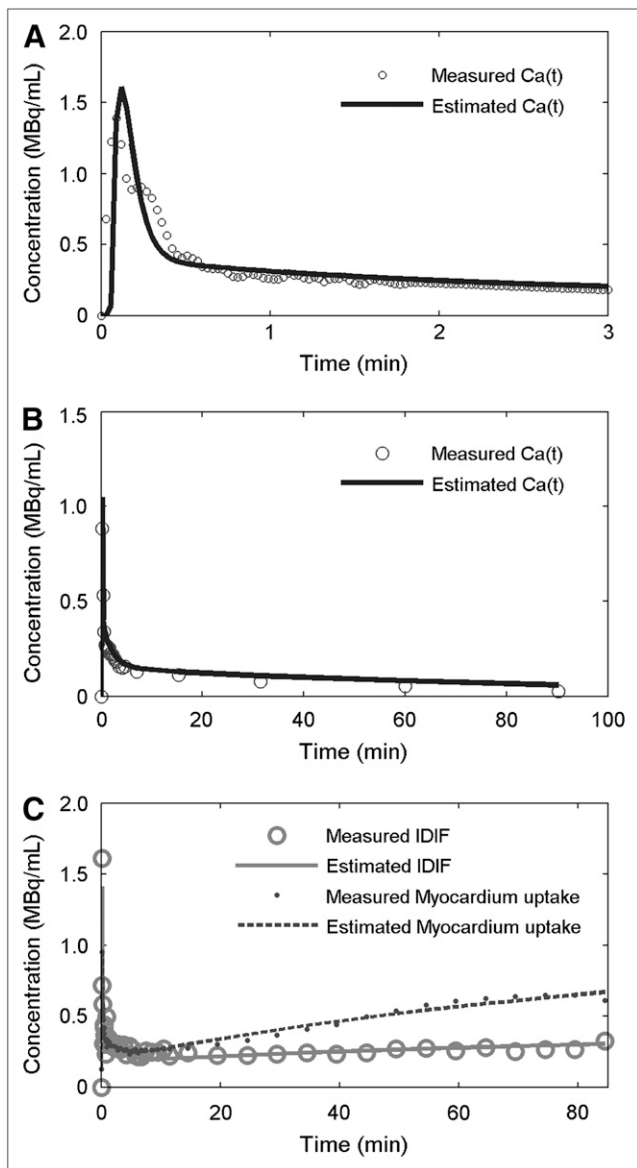


**FIGURE 3.** Estimation plots of 1 rat with the 0-sample MCIF estimation. (A) Measured input function (circles) and estimated input with the 0-sample MCIF method (solid line) for first 3 min. (B) Measured input function (circles) and estimated input with the 0-sample MCIF method (solid line) for entire scan duration. (C) Measured and model-predicted time-activity curves for IDIF and myocardium uptake. In both A and B, estimated input functions show a good agreement with the measured one. C indicates that the dual-output model can fit the data well.

the tasks of estimating the input function and  $K_i$ , greatly reducing the error for IDIFs.

Similar results can be seen in the mouse data as listed in Table 4.  $K_i$  was again highly biased when using the IDIF without correction. With the MCIF, the overall error percentage of  $K_i$  of all 3 types of tissue was  $8.0\% \pm 27.6\%$  for the 0-sample and  $2.8\% \pm 22.7\%$  for the 1-sample MCIF method, with correlation coefficients of 0.955 and 0.971, respectively. Considering the individual tissue types, myocardium had the least bias and the best precision in  $K_i$

estimates. Although the correlation was high ( $r > 0.84$ ) in all 3 types of tissue with the 0-sample MCIF, the  $t$  test detected significant biases in  $K_i$  estimates in brain and muscle ( $P < 0.05$ ). These biases were resolved by the use of the 1-sample MCIF: The significant difference was not detected in any of the 3 regions. Moreover, use of 1 sample reduced the bias and improved the precision in brain and muscle and increased the correlation coefficients of all 3 regions to  $>0.9$ . The advantages of using the blood sample are visually evident in the box plot shown in Figure 6. In summary, with  $K_i$  analysis for MCIF in mice, bias and precision are better

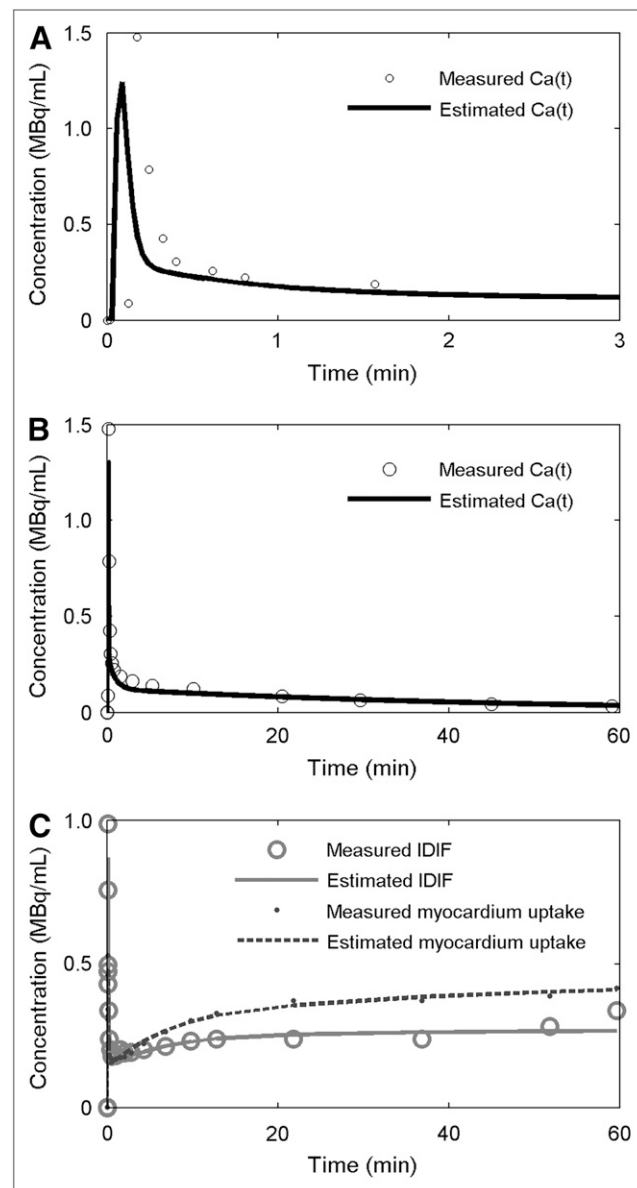


**FIGURE 4.** Estimation results of 1 mouse with the 0-sample MCIF estimation. (A) Measured input function (circles) and estimated input with 0-sample MCIF method (solid line) for first 3 min. (B) Measured input function (circles) and estimated input with 0-sample MCIF method (solid line) for entire scan duration. (C) Measured and model-predicted time-activity curves for IDIF and myocardium uptake.

**TABLE 3**  
Comparison of Ki Estimates from Measured and Estimated Input Functions from Rat Data ( $n = 20$ )

| Input function type | Statistics of Ki*            | Myocardium        | Brain             | Muscle            |
|---------------------|------------------------------|-------------------|-------------------|-------------------|
| Measured            | Estimate (1/min)             | 0.0417 ± 0.0224   | 0.0156 ± 0.0061   | 0.0023 ± 0.0012   |
| IDIF, no correction | Estimate (1/min)             | 0.0112 ± 0.0046   | 0.0027 ± 0.0046   | 0.0001 ± 0.0002   |
|                     | Error (%)                    | -69.7 ± 9.9       | -83.5 ± 21.7      | -92.9 ± 14.7      |
|                     | Corr. coefficient            | 0.886             | 0.486             | 0.183             |
|                     | <i>t</i> test <i>P</i> value | <10 <sup>-5</sup> | <10 <sup>-5</sup> | <10 <sup>-5</sup> |
| MCIF, 0-sample      | Estimate (1/min)             | 0.0410 ± 0.0229   | 0.0145 ± 0.0066   | 0.0020 ± 0.0010   |
|                     | Error (%)                    | -2.2 ± 20.8       | -5.7 ± 25.4       | -11.1 ± 33.8      |
|                     | Corr. coefficient            | 0.928             | 0.808             | 0.708             |
|                     | <i>t</i> test <i>P</i> value | 0.719             | 0.269             | 0.087             |
| MCIF, 1-sample      | Estimate (1/min)             | 0.0464 ± 0.0308   | 0.0164 ± 0.0075   | 0.0023 ± 0.0016   |
|                     | Error (%)                    | 6.1 ± 20.1        | 4.2 ± 20.3        | -0.8 ± 21.9       |
|                     | Corr. coefficient            | 0.948             | 0.861             | 0.917             |
|                     | <i>t</i> test <i>P</i> value | 0.091             | 0.329             | 0.883             |

\*Estimate (1/min) and error (%) are expressed as mean ± SD. Correlation coefficient (Corr. coefficient) and *P* values are calculated from the ( $K_{i_{mea}}$ ,  $K_{i_{est}}$ ) pairs.

than that with IDIF. Inclusion of 1 blood sample improves MCIF such that no statistically significant bias was detected.

As a less invasive alternative to using 1 late arterial blood sample, we considered substituting activity concentration in a venous sample as an approximation to that in an arterial sample. In rats, venous activity concentration differed from arterial activity concentration by  $-5.8\% \pm 13.0\%$ . Regres-

sion analysis showed a correlation coefficient of 0.944 ( $y = 0.942 \cdot x + 0.019$ , where  $y$  is the arterial activity concentration and  $x$  is the venous activity concentration), indicating that the late venous activity concentration is very close to the arterial concentration.

## DISCUSSION

The ability to quantify physiologic function with measurable and testable results in a reliable and practical manner is crucial to research. In this regard, compartment modeling has long been regarded as one of the best ways to analyze PET images. However, the blood-sampling procedure to measure the input function in small animals has been a major barrier because of its invasive nature, the small size of blood vessels, and the animals' limited blood volume. Although new and advanced devices have been proposed to measure the blood activity—such as microfluidic blood-sampling devices (15) and blood-activity monitors (20)—an invasive surgery procedure is required, making it difficult for imaging centers to include the technically demanding procedure in routine PET studies. Obtaining the input function from images using IDIFs or FA is a popular alternative as it can be done without blood sampling. IDIFs have the advantage of simplicity over FA methods but the spillover and partial-volume effects make the IDIF a highly biased estimate. Therefore, we sought to find a practical and robust method to correct for the spillover and partial-volume effect in IDIF by using simultaneous estimation to determine and correct the cross-contamination between ventricular and myocardial activities.

We compared the estimated input functions from MCIF with the inputs measured from blood samples. Our results show that the 1-sample MCIF is validated as a reliable method to estimate input functions and Ki constants. Using the extensive blood-sampling method as the reference, the AUC error

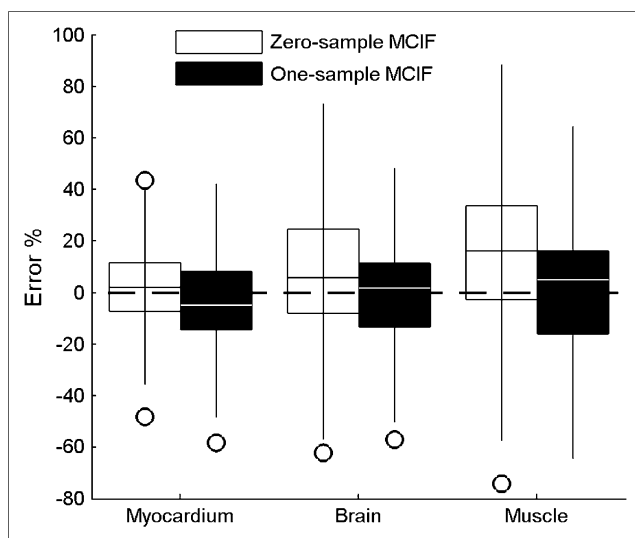


**FIGURE 5.** Box plot of Ki error percentage of the 0-sample and 1-sample MCIF estimation for rat data. Box height shows interquartile range (IQR). Median is shown as the line in the box. Whiskers indicate the quartile bounds  $\pm 1.5 \times$  IQR. Outliers that exceed this range are indicated by circles. For visual clarity, results from IDIF are not shown on this plot because the Ki with IDIF has a much higher error magnitude than the MCIF. In general, the heights of the boxes of the 1-sample MCIF are lower than those of the 0-sample MCIF. The error median is closer to 0 by the 1-sample MCIF.

**TABLE 4**  
Comparison of Ki Estimates from Measured and Estimated Input Functions from Mouse Data ( $n = 17$ )

| Input function type | Statistics of Ki*            | Myocardium        | Brain             | Muscle                 |
|---------------------|------------------------------|-------------------|-------------------|------------------------|
| Measured            | Estimate (1/min)             | 0.1381 ± 0.0655   | 0.0291 ± 0.0170   | 0.0112 ± 0.0082        |
| IDIF, no correction | Estimate (1/min)             | 0.0039 ± 0.0041   | <10 <sup>-5</sup> | <10 <sup>-5</sup>      |
|                     | Error (%)                    | -94.8 ± 7.3       | -99.9 ± 0.00      | -99.7 ± 1.11           |
|                     | Corr. coefficient            | -0.664            | -0.336            | 0.191                  |
|                     | <i>t</i> test <i>P</i> value | <10 <sup>-5</sup> | <10 <sup>-5</sup> | 3.7 × 10 <sup>-5</sup> |
| MCIF, 0-sample      | Estimate (1/min)             | 0.1321 ± 0.0696   | 0.0225 ± 0.0122   | 0.0092 ± 0.0063        |
|                     | Error (%)                    | -3.0 ± 21.7       | -13.3 ± 31.5      | -7.8 ± 29.3            |
|                     | Corr. coefficient            | 0.869             | 0.843             | 0.945                  |
|                     | <i>t</i> test <i>P</i> value | 0.487             | 0.011             | 0.016                  |
| MCIF, 1-sample      | Estimate (1/min)             | 0.1414 ± 0.0785   | 0.0268 ± 0.0168   | 0.0106 ± 0.0076        |
|                     | Error (%)                    | -1.7 ± 21.8       | -8.2 ± 17.5       | 1.6 ± 28.0             |
|                     | Corr. coefficient            | 0.924             | 0.911             | 0.969                  |
|                     | <i>t</i> test <i>P</i> value | 0.669             | 0.200             | 0.289                  |

\*Estimate (1/min) and error (%) are expressed as mean ± SD.  
Corr. coefficient = correlation coefficient.

of the 1-sample MCIF is <3% on average. Ki bias in both rats and mice is <10% and correlation coefficients are high. Most important, no significant difference was found by the *t* test in the 1-sample MCIF in both rats and mice, indicating that the 1-sample MCIF can be used as a replacement for input functions measured with extensive blood sampling. To use the 1-sample MCIF, a late venous sample, which is easy to collect, can be substituted for the arterial blood sample because late arterial and venous concentrations are very similar, as our results demonstrate. In addition, as the estimated MCIF is the whole-blood time-activity curve  $C_a$ , at least 1 blood sample must be taken to measure the hematocrit and activity fraction for conversion between  $C_p$  and  $C_a$ . This could provide the whole-blood concentration used for the simultaneous estimation in MCIF. Therefore, because 1 blood sample is simple to obtain and is necessary for hematocrit determination, we recommend using the 1-sample MCIF. On the other hand, although the 0-sample MCIF is not as accurate as 1-sample MCIF, its small bias did not reach statistical significance; thus, it may be applied in rat studies when blood sampling is infeasible or in retrospective analyses of data for which no blood samples were taken.

Compared with currently available methods for estimating input functions, MCIF has advantages. First, compared with IDIF, MCIF greatly reduces the bias by correcting for spillover and partial-volume effects. Second, compared with simultaneous estimation, MCIF has fewer parameters to estimate. Whereas the simultaneous estimation method first proposed by Wong et al. (10) models each tissue ROI according to an independent set of compartments, the MCIF method assumes that the measured heart ventricle and myocardium curves can be expressed as a weighted sum of the blood activity and the same underlying extravascular ( $C_e$ ) and metabolized ( $C_m$ ) activity concentrations. Consequently, only 2 VOIs and 1 set of  $k_1 \sim k_4$  need to be estimated for MCIF with a total number of parameters to

estimate 15, which is 10 fewer than the 25 required by the simultaneous estimation method of Wong et al. (10).

We speculate that MCIF will be improved with technological advances. For example, cardiac and respiratory gating could reduce the spillover and partial-volume effects in the IDIF (21), therefore making MCIF more robust. Similarly, image reconstruction techniques, such as a maximum a posteriori (MAP) algorithm, that accurately model the  $\gamma$ -ray transport can produce images with better resolution, therefore reducing the spillover in the IDIF (22). Those methods can be used in combination with MCIF without any conflicts. When MCIF is applied to an IDIF with less severe

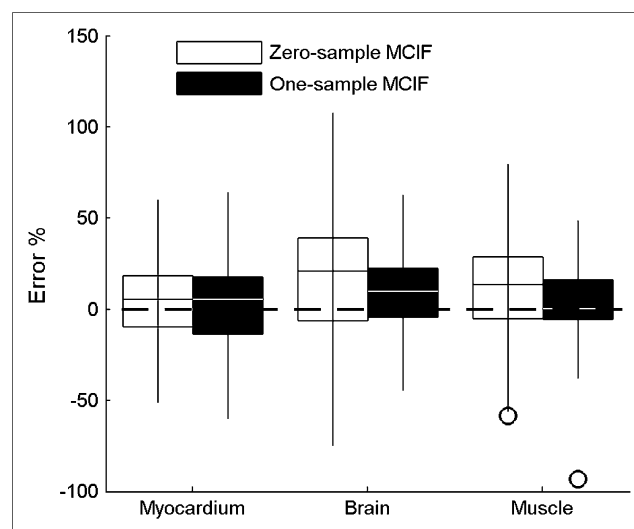


**FIGURE 6.** Box plot of Ki error percentage of the 0-sample and 1-sample MCIF estimation for mouse data. See Figure 5 legend for description of what the box height, center line, and whiskers indicate. Note significant reduction of IQR in the 1-sample MCIF. Also, the error median is closer to 0 in the 1-sample MCIF.

spillover and partial volume, MCIF should be able to estimate the input function even more accurately.

Although the MCIF method is developed and validated using  $^{18}\text{F}$ -FDG, the methodology should be applicable to other PET tracers. In particular, the output equation of the heart ventricles and myocardium would remain the same, and the configuration of the tracer kinetic model and parameter values, including initial values and bounds, would be adjusted. However, for tracers that require precise measurement of metabolites and for which a standard metabolite correction is not available, blood samples are inevitable. Otherwise, for other tracers it would be necessary to validate the adjustments in a study of a limited number of subjects wherein blood samples are collected and used for validation, as we have done here. Moreover, the MCIF should be applicable to human studies with similar adjustments and validation.

## CONCLUSION

Herein, we show that the MCIF accurately accounts for spillover and partial-volume effect for IDIF and yields an input function suitable for use in quantifying glucose metabolic rate using the  $^{18}\text{F}$ -FDG model. Specifically, we show that either 0-sample or the 1-sample MCIF has AUC error, RMSE, and  $K_i$  estimation errors that are much lower than those obtained using the uncorrected IDIF. Furthermore, the use of 1 blood sample achieves a bias of  $K_i$  estimates to a level that is not statistically significant and that is lower than the uncertainty in the  $K_i$  estimates. Therefore, MCIF can be applied to  $^{18}\text{F}$ -FDG PET small-animal imaging for modeling analysis with a minimum blood-sampling requirement. The MCIF method is incorporated into the COMKAT toolbox and is available online at <http://comkat.case.edu>, free for noncommercial research use.

## ACKNOWLEDGMENTS

This work was supported by National Institute of Health grants R33-CA-101073 and R24-CA-110943. The authors thank Dr. Henry S.C. Huang and the Crump Institute of Molecular Imaging for the courtesy of sharing mouse data with us. We thank Chandra Spring Robinson and Deborah Barkauskas for assisting with the experiments and Dr. Mark Schluchter for discussions on statistics.

## REFERENCES

1. Huang SC, Phelps ME, Hoffman EJ, Sideris K, Selin CJ, Kuhl DE. Noninvasive determination of local cerebral metabolic rate of glucose in man. *Am J Physiol.* 1980;238:E69–E82.
2. Phelps ME, Huang SC, Hoffman EJ, Selin C, Sokoloff L, Kuhl DE. Tomographic measurement of local cerebral glucose metabolic rate in humans with (F-18)2-fluoro-2-deoxy-D-glucose: validation of method. *Ann Neurol.* 1979; 6:371–388.
3. van der Weerd AP, Klein LJ, Boellaard R, Visser CA, Visser FC, Lammertsma AA. Image-derived input functions for determination of MRGlu in cardiac  $^{18}\text{F}$ -FDG PET scans. *J Nucl Med.* 2001;42:1622–1629.
4. Chen K, Bandy D, Reiman E, et al. Noninvasive quantification of the cerebral metabolic rate for glucose using positron emission tomography,  $^{18}\text{F}$ -fluoro-2-deoxyglucose, the Patlak method, and an image-derived input function. *J Cereb Blood Flow Metab.* 1998;18:716–723.
5. Ohtake T, Kosaka N, Watanabe T, et al. Noninvasive method to obtain input function for measuring tissue glucose utilization of thoracic and abdominal organs. *J Nucl Med.* 1991;32:1432–1438.
6. Yee SH, Jerabek PA, Fox PT. Non-invasive quantification of cerebral blood flow for rats by microPET imaging of  $^{15}\text{O}$  labelled water: the application of a cardiac time-activity curve for the tracer arterial input function. *Nucl Med Commun.* 2005; 26:903–911.
7. Green LA, Gambhir SS, Srinivasan A, et al. Noninvasive methods for quantitating blood time-activity curves from mouse PET images obtained with fluorine-18-fluorodeoxyglucose. *J Nucl Med.* 1998;39:729–734.
8. Kim J, Herrero P, Sharp T, et al. Minimally invasive method of determining blood input function from PET images in rodents. *J Nucl Med.* 2006;47:330–336.
9. Meyer PT, Circiumaru V, Cardi CA, Thomas DH, Bal H, Acton PD. Simplified quantification of small-animal [ $^{18}\text{F}$ ]FDG PET studies using a standard arterial input function. *Eur J Nucl Med Mol Imaging.* 2006;33:948–954.
10. Wong KP, Feng D, Meikle SR, Fulham MJ. Simultaneous estimation of physiological parameters and the input function: in vivo PET data. *IEEE Trans Inf Technol Biomed.* 2001;5:67–76.
11. Salinas CA, Pagel MD, Muzic RF Jr. Measurement of arterial input functions in rats. Paper presented at: Annual Meeting of the Society for Molecular Imaging; September 11, 2004; St. Louis, MO.
12. Huang S-C. Mouse quantitation program (MQP). Available at: <http://dragon.nuc.ucla.edu/mqp/index.html>. Accessed December 7, 2007.
13. Huang SC, Wu HM, Truong D, et al. A public domain dynamic mouse FDG microPET image data set for evaluation and validation of input function derivation methods. Paper presented at: Nuclear Science Symposium Conference Record, 2006. Institute of Electrical and Electronics Engineers; November 3, 2006; San Diego, CA.
14. Weber B, Burger C, Biro P, Buck A. A femoral arteriovenous shunt facilitates arterial whole blood sampling in animals. *Eur J Nucl Med Mol Imaging.* 2002; 29:319–323.
15. Wu HM, Sui G, Lee CC, et al. In vivo quantitation of glucose metabolism in mice using small-animal PET and a microfluidic device. *J Nucl Med.* 2007; 48:837–845.
16. Feng D, Huang SC, Wang X. Models for computer simulation studies of input functions for tracer kinetic modeling with positron emission tomography. *Int J Biomed Comput.* 1993;32:95–110.
17. Muzic RF Jr, Christian BT. Evaluation of objective functions for estimation of kinetic parameters. *Med Phys.* 2006;33:342–353.
18. Muzic RF Jr, Cornelius S. COMKAT: compartment model kinetic analysis tool. *J Nucl Med.* 2001;42:636–645.
19. Coleman TF, Li Y. An interior trust region approach for nonlinear minimization subject to bounds. *SIAM J Optim.* 1996;6:418–445
20. Convert L, Morin-Brassard G, Cadorette J, Archambault M, Bentourkia M, Lecomte R. A new tool for molecular imaging: the microvolumetric beta blood counter. *J Nucl Med.* 2007;48:1197–1206.
21. Yang Y, Rendig S, Siegel S, Newport DF, Cherry SR. Cardiac PET imaging in mice with simultaneous cardiac and respiratory gating. *Phys Med Biol.* 2005; 50:2979–2989.
22. Stout D, Kreissl MC, Wu H-M, Schelbert HR, Huang S-C. Left ventricular blood TAC quantitation with microPET imaging in mice using MAP, FBP and blood sampling. Paper presented at: Nuclear Science Symposium Conference Record, 2005. Institute of Electrical and Electronics Engineers; October 28, 2006; San Juan, Puerto Rico.